Nuclear EMC Effect for Electron and Neutrino Scattering

Sergey Kulagin

Institute for Nuclear Research, Moscow

Talk at the workshop
Neutrino-Nucleus Interactions for Current and Next Generation Neutrino Oscillation Experiments
Seattle, December 9, 2013

Outline

- Overview of data on nuclear effects in lepton deep inelastic scattering (DIS).
- Overview of a model of nuclear DIS
  - Sketch of basic physics mechanisms of nuclear corrections in different kinematic regions
  - Trying to put those mechanisms together in a model
  - Discuss performance and predictions of the model
- New data (JLab E03-103, HERMES) and model predictions
- Predictions for DY data (E772 and E866 experiments).
- Predictions for neutrino DIS

Data on nuclear effects in DIS

- Data on nuclear effects in DIS are available in the form of the ratio $\mathcal{R}(A/B) = \sigma_A(x,Q^2)/\sigma_B(x,Q^2)$ or F_2^A/F_2^B.
- Data for nuclear targets from ^{2}H to ^{208}Pb
- Fixed-target experiments with e/μ:
  - Muon beam at CERN (EMC, BCDMS, NMC) and FNAL (E665).
  - Electron beam at SLAC (E139, E140), HERA (HERMES), JLab (E03-103).
- Kinematics and statistics:
  Data covers the region $10^{-4} < x < 1.5$ and $0 < Q^2 < 150\,\mathrm{GeV}^2$. About 800 data points for the nuclear ratios $\mathcal{R}(A/B)$ with $Q^2 > 1$ GeV^2.
- Additional information on nuclear effects for antiquarks comes from Drell-Yan production from fixed-target experiments at FNAL (E772, E866).
- Neutrino data on DIS cross sections on nuclear targets ^{2}H, ^{20}Ne, ^{12}C, ^{56}Fe, ^{207}Pb from CERN (BEBC, CDHS, CHORUS, NOMAD) and FNAL (CCFR, NuTeV).
- Upcoming measurement of the nuclear ratios from MINERvA in a shallow inelastic region.

Data on the EMC ratios show pronounced A dependence of the ratios $\mathcal{R}(A/D)$ and a weak Q^2 dependence of nuclear effects. Characteristic nuclear effects vs. the Bjorken x – ~~neutrino~~ structure function strength oscillation

- Suppression (shadowing) at small x ($x < 0.05$).

- Enhancement (antishadowing) at $0.1 < x < 0.25$.

- A well with a minimum at $x \sim 0.6 \div 0.75$ (EMC effect).

- Enhancement at large values of $x > 0.75 \div 0.8$ (Fermi motion region).

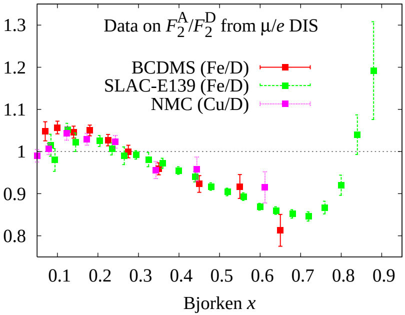

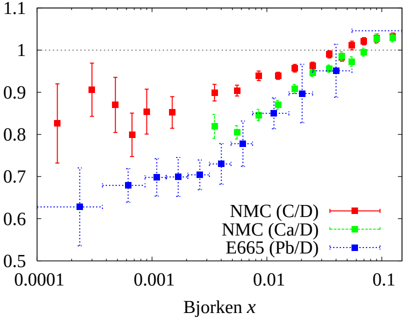

Recent data from JLAB

E03-103 experiment at Jlab *J.Seely et.al., PRL103,202301,2009*:

- Nuclear target ratios: ^{12}C/^{2}H, ^{9}Be/^{2}H, ^{4}He/^{2}H, ^{3}He/^{2}H.
- Kinematics: Beam energy $E = 5.011$ and 5.766 GeV. Scattering angles are $32,\ 36,\ 40,\ 46,\ 50$ grad.
- About 150 data points were reported in the region $0.3 < x < 0.9$ and $2.8 < Q^2 < 7$ GeV^2.
- Statistics of E03-103 at large x is significantly higher than that from previous measurements.

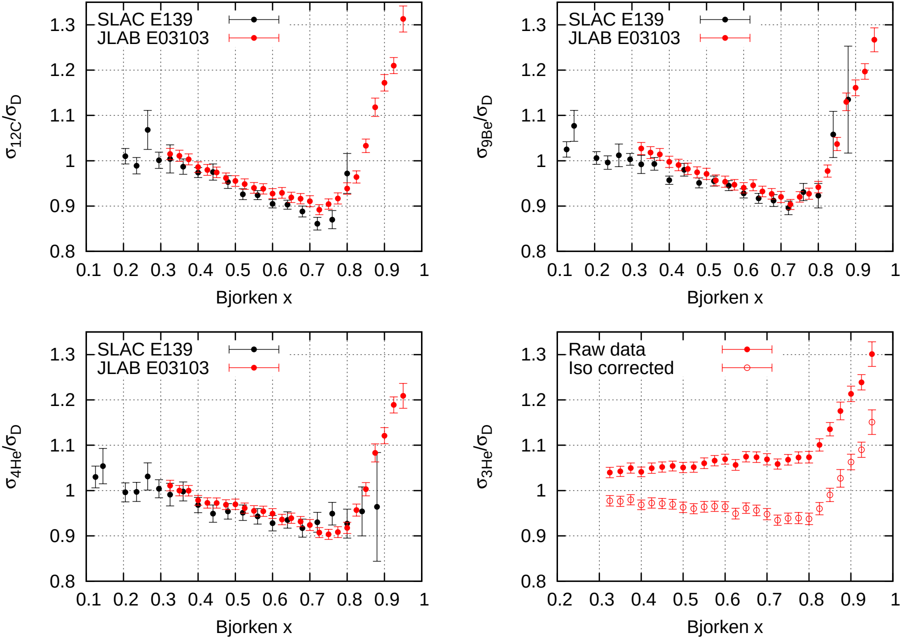
SLAC E139
JLAB E03103
σ_{12C}/σ_D
σ_{9Be}/σ_D
σ_{4He}/σ_D
Raw data
Iso corrected
σ_{3He}/σ_D
Bjorken x

Consistency of different experiments

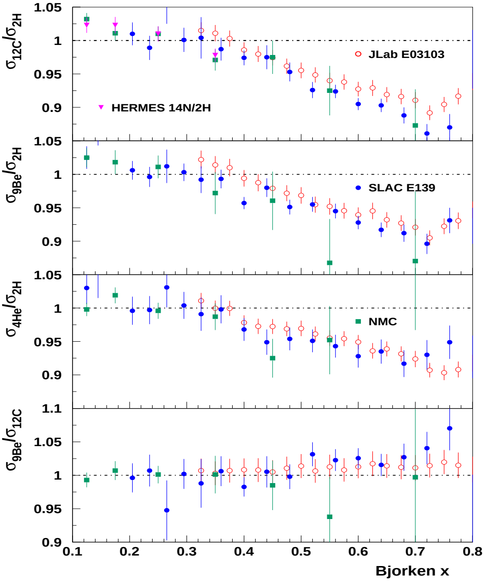

- Shapes of all nuclear cross-section ratios are consistent
- Evaluate χ^2 for each pair of experiments in coarse x-bins within the overlap region of the data sets
- Consistent overall normalization for SLAC E139, NMC and HERMES data sets
- The new JLab E03-103 data is systematically above previous measurements resulting in a $\chi^2/d.o.f. = 42.7/12$ with respect to SLAC E139 data on the same targets
- An overall normalization factor 0.98 for all JLab E03-103 points improves the statistical consistency with SLAC E139 data to $\chi^2/d.o.f. = 8.8/12$

DIS space-time scales

The analysis of characteristic space-time scales involved into DIS helps to approach the nuclear physics of the process. Typical DIS space-time regions in the target rest frame as derived from uncertainty principle

- DIS proceeds near the light cone: $t^2 - z^2 \sim Q^{-2}$ and $r_\perp \sim Q^{-1}$.
- Characteristic DIS time and longitudinal distance $t \sim z \sim L = (Mx)^{-1}$ NOT small in hadronic scale (in the target rest frame) $\Rightarrow$ the reason for nuclear effects to survive even at high Q^2.

L has to be compared with average distance between bound nucleons $d = (3/4\pi\rho)^{1/3} \sim 1.2\,$Fm ($\rho$ is the nucleon number density in central region of heavy nuclei). This suggests two different kinematical regions:

- $L_I < d$ $(x > 0.2)$ $\Rightarrow$ Nuclear DIS $\approx$ incoherent sum of contributions from bound nucleons.
- $L_I \gg d$ $(x \ll 0.2)$ $\Rightarrow$ Coherent effects of interactions with a few nucleons are important.

Impulse approximation

$$W^A_{\mu\nu}(P_A,q)=\sum_{\tau=p,n}\int \mathrm{d}^4p\ \mathrm{Tr}\left[\widehat{\mathcal{W}}^\tau_{\mu\nu}(p,q)\mathcal{A}^\tau(p;A)\right],$$

$$\mathcal{A}^\tau_{\alpha\beta}(p;A)=\int \mathrm{d}t\mathrm{d}^3\boldsymbol{r}e^{ip_0t-i\boldsymbol{p}\cdot\boldsymbol{r}}\langle A|\overline{\Psi}^\tau_\beta(t,\boldsymbol{r})\,\Psi^\tau_\alpha(0)|A\rangle$$

- $\Psi^\tau_\alpha(t,\boldsymbol{r})$ the nucleon Dirac field operator.
- The off-shell nucleon tensor $\widehat{\mathcal{W}}_{\mu\nu}(p,q)$ is the matrix in the Dirac space.

On the mass shell $p^2=M^2$, averaging $\widehat{\mathcal{W}}_{\mu\nu}(p,q)$ over the nucleon polarizations we obtain the nucleon tensor given in terms of 2 structure functions

$$W^\tau_{\mu\nu}(p,q)=\frac{1}{2}\mathrm{Tr}\left[(\not{p}+M)\widehat{\mathcal{W}}^\tau_{\mu\nu}(p,q)\right]=\widetilde{g}_{\mu\nu}F_1+\widetilde{p}_\mu\widetilde{p}_\nu F_2/p\cdot q$$

How many structure function do we have off-mass-shell $p^2\neq M^2$? Expand in the Dirac basis:

$$\widehat{W}_{\mu\nu}=\sum_n W^n_{\mu\nu}\Gamma_n$$

$$\Gamma_n=I,\gamma^\alpha,\sigma^{\alpha\beta},\gamma^\alpha\gamma_5,\gamma_5$$

Require the symmetry under P and T transformations AND keeping ONLY current-conserving terms ($q_\mu W_{\mu\nu} = 0$) we have 7 independent structure functions.

$$
\begin{aligned}
2\,\widehat{\mathcal{W}}^{\mathrm{sym}}_{\mu\nu}(p,q) \quad = \quad & -\widetilde{g}_{\mu\nu}\left(\frac{f_1^{(0)}}{M} + \frac{f_1^{(1)}\,\not{p}}{M^2} + \frac{f_1^{(2)}\,\not{q}}{p\cdot q}\right) \\
& + \frac{\widetilde{p}_\mu \widetilde{p}_\nu}{p\cdot q}\left(\frac{f_2^{(0)}}{M} + \frac{f_2^{(1)}\,\not{p}}{M^2} + \frac{f_2^{(2)}\,\not{q}}{p\cdot q}\right) + \frac{f_2^{(3)}}{p\cdot q}\,\widetilde{p}_{\{\mu}\widetilde{g}_{\nu\}\alpha}\gamma^\alpha,
\end{aligned}
$$

Contribution of each of these structure functions is goverened by corresponding matrix element $\langle\overline{\Psi}\Gamma_n\Psi\rangle$.
On the mass shell $p^2 = M^2$ we only have 2 independent structure functions

$$
\begin{aligned}
F_1 &= f_1^{(0)} + f_1^{(1)} + f_1^{(2)}, \\
F_2 &= f_2^{(0)} + f_2^{(1)} + f_2^{(2)} + f_2^{(3)}
\end{aligned}
$$

Weak binding approximation

Assume the ground state to be nonrelativistic:

- $|\boldsymbol{p}| \ll M, \||p_0 - M| \ll M$
- No strong scalar and vector fields in nuclei

Reduce the four-component relativistic field Ψ to a two-component nonrelativistic operator ψ

$$\Psi(\boldsymbol{p}, t) = e^{-iMt} Z \begin{pmatrix} \psi(\boldsymbol{p}, t) \\ (\boldsymbol{\sigma} \cdot \boldsymbol{p}/2M)\, \psi(\boldsymbol{p}, t) \end{pmatrix}, \qquad Z = 1 - \frac{\boldsymbol{p}^2}{8M^2}$$

The renormalization operator Z provides a correct normalization of the nonrelativistic two-component nucleon field ψ:
$\int \mathrm{d}^3 p \Psi^\dagger \Psi = \int \mathrm{d}^3 p \psi^\dagger \psi$ to order $\boldsymbol{p}^2/M^2$.
Separate the nucleon mass M from the energy p_0, $p = (M + \varepsilon, \boldsymbol{p})$. Examine and reduce all the Lorentz–Dirac structures of $\widehat{W}_{\mu\nu}$. The result to order ε/M and $\boldsymbol{p}^2/M^2$ can be summarized as

$$\frac{1}{M_A}\,\mathrm{Tr}\left(\mathcal{A}(p;A)\,\widehat{\mathcal{W}}_{\mu\nu}(p,q)\right) = \frac{1}{M+\varepsilon}\,\mathcal{P}(\varepsilon,\boldsymbol{p})\,W_{\mu\nu}(p,q),$$

$$\mathcal{P}(\varepsilon,\boldsymbol{p}) = \int \mathrm{d}t\,e^{-i\varepsilon t}\langle\psi^\dagger(\boldsymbol{p},t)\psi(\boldsymbol{p},0)\rangle$$

$$\frac{W^A_{\mu\nu}(P_A,q)}{M_A} = \sum_{\tau=p,n}\int\frac{\mathrm{d}^4p}{M+\varepsilon}\mathcal{P}^\tau(\varepsilon,\boldsymbol{p})W^\tau_{\mu\nu}(p,q),$$

$$F_1(x,Q^2,p^2) = f_1^{(0)}\left(1+\frac{p^2-M^2}{2M^2}\right)+f_1^{(1)}\frac{p^2}{M^2}+f_1^{(2)},$$

$$F_2(x,Q^2,p^2) = f_2^{(0)}\left(1+\frac{p^2-M^2}{2M^2}\right)+f_2^{(1)}\frac{p^2}{M^2}+f_2^{(2)}+f_2^{(3)}$$

Comments:

- In the nonrelativistic limit to order $\boldsymbol{p}^2/M^2 \sim \varepsilon/M$ we have a factorization of the high-energy amplitude $W_{\mu\nu}$ from the nuclear spectral function $\mathcal{P}$ which describes the low-energy part of the problem.
- In the vicinity of the mass shell the hadronic tensor has the same number of independent structure functions as on the mass shell.
- The bound nucleon structure functions explicitly depend on p^2. This dependence is generaly present in the scaling limit.

Structure functions in Impulse Approximation)

In impulse approximation (IA) the basic corrections are due to the nucleon momentum distribution and its energy spectrum:

$$F_2^A(x,Q^2) = \int \mathrm{d}^4 p\, \mathcal{P}_A(p) \left(1 + \frac{p_z}{M}\right) F_2^N(x', Q^2, p^2),$$

$$x = \frac{Q^2}{2Mq_0}, \quad x' = \frac{Q^2}{2p\cdot q} \approx \frac{M\,x}{p_0 + p_z}$$

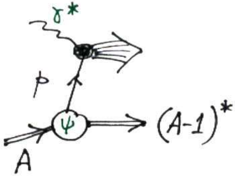

Bound nucleon momentum and binding energy effect is driven by nuclear spectral function, which describes probability to find a bound nucleon with momentum $\boldsymbol{p}$ and energy $p_0 = M + \varepsilon$:

$$\mathcal{P}_A(p) = \sum_{(A-1)_n} \left|\langle (A-1)_n, -\boldsymbol{p}|\psi(0)|A\rangle\right|^2 \delta(\varepsilon + E_n(A-1) - E_0(A)).$$

Nuclear spectral function

The nuclear spectral function describes probability to find a bound nucleon with momentum $\boldsymbol{p}$ and energy $p_0 = M + \varepsilon$:

$$\begin{aligned}
\mathcal{P}(\varepsilon, \boldsymbol{p}) &= \int \mathrm{d}t\, e^{-i\varepsilon t} \langle \psi^\dagger(\boldsymbol{p}, t)\psi(\boldsymbol{p}, 0)\rangle \\
&= \sum_{(A-1)_n} \left|\langle (A-1)_n, -\boldsymbol{p}|\psi(0)|A\rangle\right|^2 2\pi\delta\left(\varepsilon + E_n^{A-1}(\boldsymbol{p}) - E_0^A\right)
\end{aligned}$$

The nuclear spectral function determines the rate of nucleon removal reactions such as $(e, e'p)$. For low separation energies and momenta, $|\varepsilon| < 50\,\mathrm{MeV}$, $p < 300\,\mathrm{MeV/c}$, the observed spectrum is similar to that predicted by the mean-field model. The mean-field model spectral function is given by the wave functions and energies of the occupied levels in the mean field

$$\mathcal{P}_{\mathrm{MF}}(\varepsilon, \boldsymbol{p}) = \sum_{\lambda<\lambda_F} n_\lambda |\phi_\lambda(\boldsymbol{p})|^2 \delta(\varepsilon - \varepsilon_\lambda)$$

Two-component model

As nuclear excitation energy becomes higher the mean-field model becomes less accurate.

- The peaks corresponding to the single-particle levels acquire a finite width (fragmentation of deep-hole states).
- High-energy and high-momentum components of nuclear spectrum can not be described in the mean-field model and driven by correlation effects in nuclear ground state as witnessed by numerous studies.

$$\mathcal{P} = \mathcal{P}_{\mathrm{MF}} + \mathcal{P}_{\mathrm{cor}}$$

The correlated part is determined by $(A-1)^*$ excited states with one or more nucleons in the continuum. Following *Ciofi degli Atti & Simula, 1996* we assume the dominance of configurations with a correlated nucleon-nucleon pair and remaining $A-2$ nucleons moving with low center-of-mass momentum

$$|A-1, -\boldsymbol{p}\rangle \approx \psi^\dagger(\boldsymbol{p}_1)|(A-2)^*, \boldsymbol{p}_2\rangle \delta(\boldsymbol{p}_1 + \boldsymbol{p}_2 + \boldsymbol{p}).$$

The matrix element can thus be given in terms of the wave function of the nucleon-nucleon pair embeded into nuclear environment. We assume factorization into relative and center-of-mass motion of the pair

$$\langle (A-2)^*, \boldsymbol{p}_2 \,|\psi(\boldsymbol{p}_1)\psi(\boldsymbol{p})|\, A\rangle \approx C_2 \psi_{\mathrm{rel}}(\boldsymbol{k})\psi_{\mathrm{CM}}^{A-2}(\boldsymbol{p}_{\mathrm{CM}})\delta(\boldsymbol{p}_1+\boldsymbol{p}_2+\boldsymbol{p}),$$

where ψ_{rel} is the wave function of the relative motion in the nucleon-nucleon pair with relative momentum $\boldsymbol{k}=(\boldsymbol{p}-\boldsymbol{p}_1)/2$ and ψ_{CM} is the wave function of center-of-mass (CM) motion of the pair in the field of $A-2$ nucleons, $\boldsymbol{p}_{\mathrm{CM}}=\boldsymbol{p}_1+\boldsymbol{p}$. The factor C_2 describes the weight of the two-nucleon correlated part in the full spectral function.

$$\mathcal{P}_{\mathrm{cor}}(\varepsilon,\boldsymbol{p}) \approx n_{\mathrm{cor}}(\boldsymbol{p}) \left\langle \delta\left(\varepsilon + \frac{(\boldsymbol{p}+\boldsymbol{p}_{A-2})^2}{2M} + E_{A-2} - E_A\right)\right\rangle_{A-2}$$

The full spectral function can be approximated by a sum of the MF and the correlation parts $\mathcal{P}=\mathcal{P}_{\mathrm{MF}}+\mathcal{P}_{\mathrm{cor}}$.

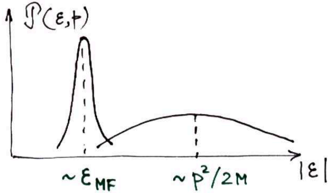

Average separation and kinetic energies

Normalization of MF and cor parts:

$$A^{-1}\int \mathrm{d}\varepsilon \mathrm{d}^3p \mathcal{P}_{\mathrm{MF}} = 0.8, \quad A^{-1}\int \mathrm{d}\varepsilon \mathrm{d}^3p \mathcal{P}_{\mathrm{cor}} = 0.2$$

Average separation $\langle\varepsilon\rangle$ and kinetic $\langle T\rangle$ energies are related by the Koltun sum rule (exact relation for nonrelativistic system with two-body forces)

$$\langle\varepsilon\rangle + \langle T\rangle = 2\varepsilon_B,$$

where $\varepsilon_B = E_0^A/A$ is nuclear binding energy per bound nucleon

$$\langle\varepsilon\rangle = A^{-1}\int [\mathrm{d}p]\mathcal{P}(\varepsilon,\boldsymbol{p})\varepsilon,$$
$$\langle T\rangle = A^{-1}\int [\mathrm{d}p]\mathcal{P}(\varepsilon,\boldsymbol{p})\frac{\boldsymbol{p}^2}{2M}.$$

Nuclear binding, separation and kinetic energies

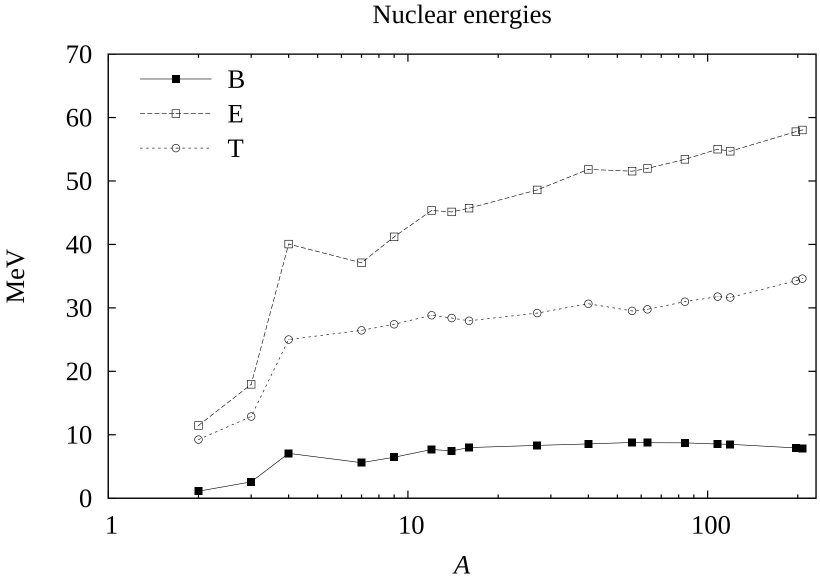

EMC effect in impulse approximation

- Fermi motion qualitatively describes the trend of data at $x > 0.7$.
- Binding correction is important and brings the calculation closer to data in the dip region.
- However, even realistic nuclear spectral function fails to explain the slope and the position of the minimum.

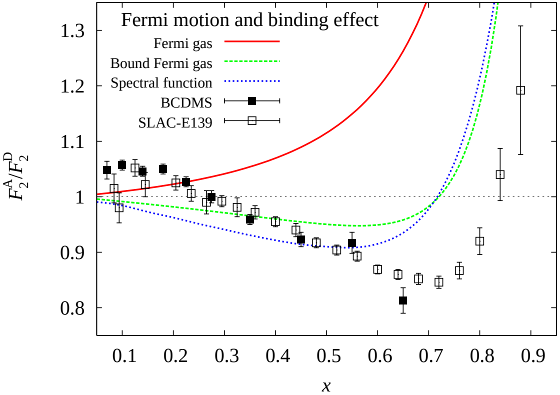

Impulse Approximation should be corrected for a number of effects.

Nucleon off-shell effect

Bound nucleons are off-mass-shell $p^2 = (M+\varepsilon)^2 - \boldsymbol{p}^2 < M^2$. In off-shell region nucleon structure functions depend on additional variable $F_2(x, Q^2, p^2)$.
The nucleon virtuality parameter $v = (p^2 - M^2)/M^2$ is small (average virtuality $v \sim -0.15$ for ^{56}Fe). Expand $F_2(x, Q^2, p^2)$ in series in v:

$$F_2^N(x, Q^2, p^2) = F_2^N(x, Q^2)\big(1 + \delta f_2(x, Q^2)(p^2 - M^2)/M^2\big)$$

- $\delta f_2(x, Q^2)$ is a new structure function that describes modification of the off-shell nucleon PDFs in the vicinity of the mass shell.
- Off-shell correction is closely related to modification of the nucleon PDFs in nuclear environment.

Average virtuality (offshellness) of a bound nucleon

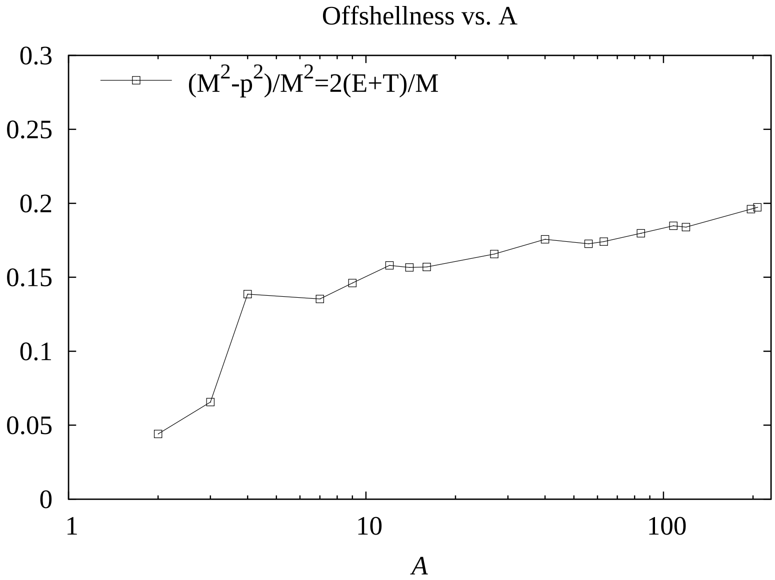

Nuclear pion effect

Leptons can scatter on nuclear meson field which mediate interaction between bound nucleons. This process generate a pion correction to nuclear sea quark distribution

$$\delta F_i^{\pi/A}(x,Q^2) = \int_x \mathrm{d}y f_{\pi/A}(y) F_i^{\pi}(x/y,Q^2)$$

- Contribution from nuclear pions (mesons) is important to balance nuclear light-cone momentum $\langle y\rangle_\pi + \langle y\rangle_N = 1$.
- The nuclear pion distribution function is localized in a region $y < p_F/M \sim 0.3$. For this reason the pion correction to nuclear (anti)quark distributions is localized at $x < 0.3$.
- The magnitude of the correction is driven by average number of "nuclear pion excess" $n_\pi = \int \mathrm{d}y\, f_{\pi/A}(y)$ and $n_\pi/A \sim 0.1$ for a heavy nucleus like 56Fe.

Coherent nuclear corrections

Two different mechanisms of DIS:

(I) Quasielastic scattering off bound quark. This process dominates at intermediate and large values of x and the structure functions are determined by the quark wave (spectral) functions.

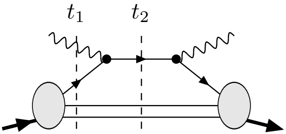

Nuclear effects arise due to averaging with nucleon distributions in a nucleus.

(II) Conversion $\gamma^* \to q\bar{q}$ with subsequent propagation of a $q\bar{q}$ state. This process dominates at small x since the life time of a $q\bar{q}$ state grows as $(Mx)^{-1}$. The structure functions are determined by quark scattering amplitudes.

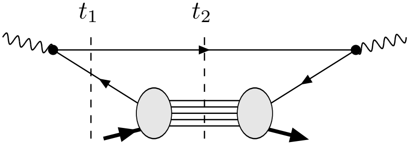

Nuclear effects arise due to propagation of $q\bar{q}$ state in nuclear environment.

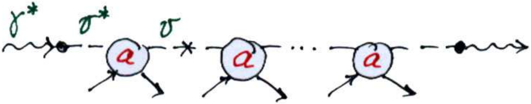

The multiple scattering series can be summed up in the Glauber-Gribov approach. For a large A we have

$$\delta\mathcal{R} = \frac{\delta F_2^{\text{coh}}}{F_2^N} \approx \frac{\delta\sigma^{\text{coh}}}{\sigma} = \operatorname{Im}\left[ia^2\mathcal{C}_2^A(a)\right] / \operatorname{Im} a,$$

$$\mathcal{C}_2^A(a) = \int_{z_1<z_2} \mathrm{d}^2\boldsymbol{b}\,\mathrm{d}z_1\mathrm{d}z_2\,\rho_A(\boldsymbol{b},z_1)\rho_A(\boldsymbol{b},z_2)\exp\left[i\int_{z_1}^{z_2}\mathrm{d}z'\,(a\,\rho_A(\boldsymbol{b},z')-k_L)\right].$$

where $\rho_A(\boldsymbol{r})$ is the nuclear number density and $a = \sigma(i+\alpha)/2$ is a scattering amplitude in forward direction, $k_L = Mx(1+m_v^2/Q^2)$ is longitudinal momentum transfer in the process $v^* \to v$ which accounts for the life time of intermediate $q\bar{q}$ (hadronic) state. The presence of k_L suppresses nuclear mult. scat. effect as x increases.

Model *S.K. & R.Petti, Nucl. Phys. A765 (2006) 126*

A quantitative model for nuclear structure functions

$$F_i^A = F_i^{p/A} + F_i^{n/A} + \delta_\pi F_i + \delta_{\mathsf{coh}} F_i$$

- $F_i^{p/A}$ and $F_i^{n/A}$ are bound proton and neutron structure functions with Fermi motion, binding and off-shell effects calculated using realistic nuclear spectral function.
- $\delta_\pi F_i^A$ and $\delta_{\mathsf{coh}} F_i^A$ are nuclear pion and shadowing corrections.

In actual calculations we use:

- Free proton and neutron structure functions computed in NNLO pQCD + TMC + HT using phenomenological PDFs and HTs from fits to DIS data by *S.Alekhin*.
- Realistic nuclear spectral function which includes the mean-field as well as the correlated part.
- Nuclear pion correction as a convolution of nuclear pion distribution function with pion PDFs.
- Coherent nuclear corrections are calculated using Glauber-Gribov multiple scattering theory in terms of effective amplitude a_T.

Analysis of nuclear ratios (EMC effect)

Strategy: Parameterize unknown off-shell function $f_2(x)$ and effective scattering amplitude a_T. Calculate nuclear structure functions, test with data and extract parameters from data.

- We study the data from e/μ DIS in the form of ratios $R_2(A/B) = F_2^A/F_2^B$ for a variaty of targets. The data are available for $A/^2H$ and $A/^{12}C$ ratios.
- We perform a fit to minimize $\chi^2 = \sum_{\text{data}}(\mathcal{R}_2^{exp} - \mathcal{R}_2^{th})^2/\sigma^2(\mathcal{R}_2^{exp})$ with σ the experimental uncertainty of $\mathcal{R}_2^{exp}$. We use data with $Q^2 > 1$ GeV^2. The nuclear ratios used in our analysis (overall about 560 points available before 1996):

^{4}He/D	^{7}Li/D	^{9}Be/D
^{12}C/D	^{27}Al/D	^{27}Al/^{12}C
^{40}Ca/D	^{40}Ca/^{12}C	
^{56}Fe/D	^{63}Cu/D	^{56}Fe/^{12}C
^{108}Ag/D	^{119}Sn/^{12}C	
^{197}Au/D	^{207}Pb/D	^{207}Pb/^{12}C

- Verify the model by comparing the calculations with data not used in analysis.

Parameters of the model

- Off-shell structure function $\delta f_2(x) = C_N(x-x_1)(x-x_0)(h-x)$
  - From preliminary studies we observe that h is fully correlated with x_0, i.e. $h = 1 + x_0$.
  - C_N, x_0, x_1 are independent ajustable parameters.
- Effective amplitude

$$\bar{a}_T = \bar{\sigma}_T(i+\alpha)/2, \quad \bar{\sigma}_T = \sigma_1 + \frac{\sigma_0 - \sigma_1}{1 + Q^2/Q_0^2}$$

  - Parameters $\sigma_0 = 27\,\text{mb}$ and $\alpha = -0.2$ were fixed in order to match the vector meson dominance model predictions at low Q.
  - Parameter $\sigma_1 = 0$ fixed (preferred by preliminary fits and fixed in the final studies).
  - Q_0^2 is adjustable scale parameter controlling transition between low and high Q regimes.

Results

- The x, Q^2 and A dependencies of the nuclear ratios are reproduced for all studied nuclei (^{4}He to ^{208}Pb) in a 4-parameter fit with $\chi^2/\text{d.o.f.} = 459/556$.
- Global fit to all data is consistent with the fits to different subsets of nuclei (light, medium, heavy nuclei).
- Parameters of the off-shell function δf and effective amplitude a_T are determined with a good accuracy.

For detailed discussion and comparison with data see *S.K. & R.P., Nucl Phys A765(2006)126*.

^{4}He/D

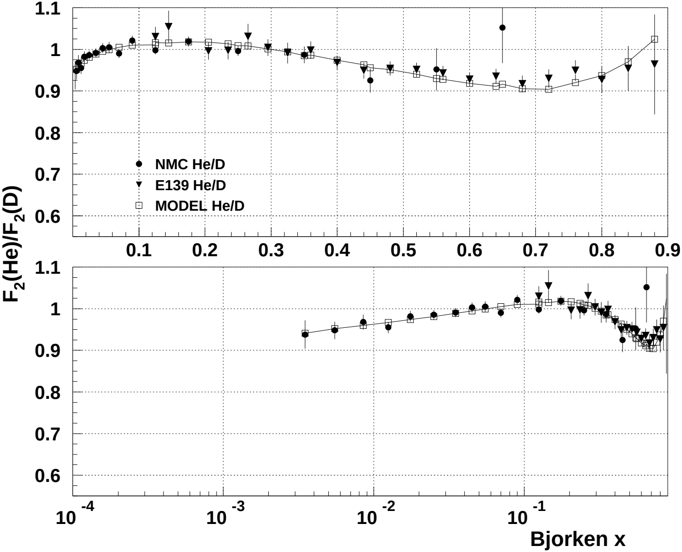

1.1
1
0.9
0.8
0.7
0.6
0.1
0.2
0.3
0.4
0.5
0.6
0.7
0.8
0.9
NMC He/D
E139 He/D
MODEL He/D
$F_2(He)/F_2(D)$
10^{-4}
10^{-3}
10^{-2}
10^{-1}
Bjorken x

^{197}Au/D & ^{207}Pb/D

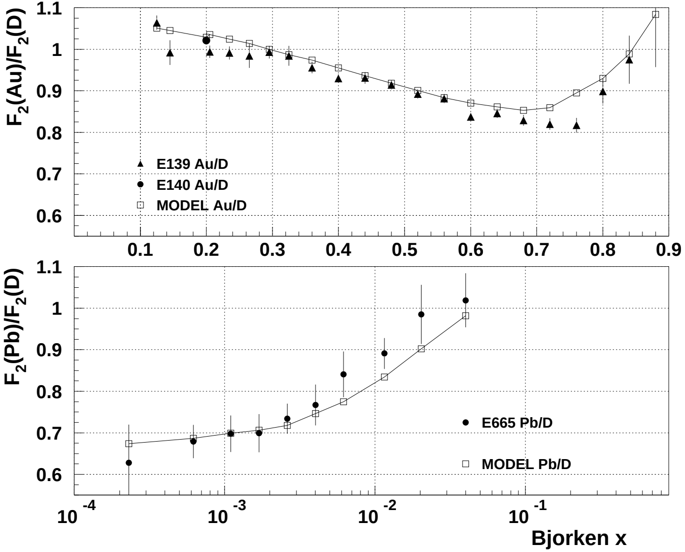

Off-shell function

$$\delta f(x) = C_N(x - x_1)(x - x_0)(1 + x_0 - x)$$
$$C_N = 8.1 \pm 0.3 \pm 0.5$$
$$x_0 = 0.448 \pm 0.005 \pm 0.007$$
$$x_1 = 0.05$$

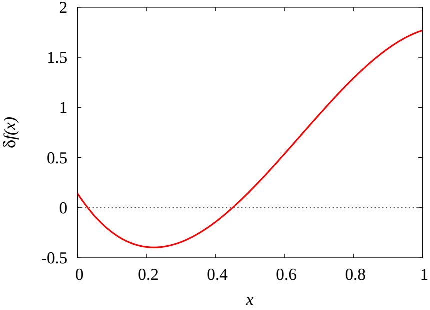

- The function $\delta f(x)$ provides a measure of the modification of quark distributions in a bound nucleon.
- The off-shell effect results in the enhancement of the structure function for $x_1 < x < x_0$ and depletion for $x < x_1$ and $x > x_0$.

Effective cross section

$\sigma_T = \sigma_0/(1 + Q^2/Q_0^2)$ with
$\sigma_0 = 27$ mb and
$Q_0^2 = 1.43 \pm 0.06 \pm 0.195$ GeV^2
provides a good fit to existing DIS data on nuclear shadowing for $Q^2 < 20$ GeV^2.

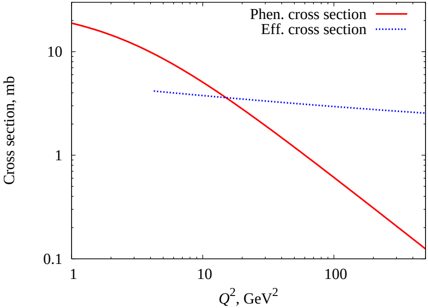

The cross section at high Q^2 is not constrained by data. Effective cross section from normalization of the nuclear valence quark distribution:

$$\delta N_{\rm val}^{\rm OS} + \delta N_{\rm val}^{\rm NS} = 0.$$

Numeric solution to this equation is shown by blue curve.

Different nuclear effects for $^{197}\mathrm{Au}$ at $Q^2 = 10\,\mathrm{GeV}^2$

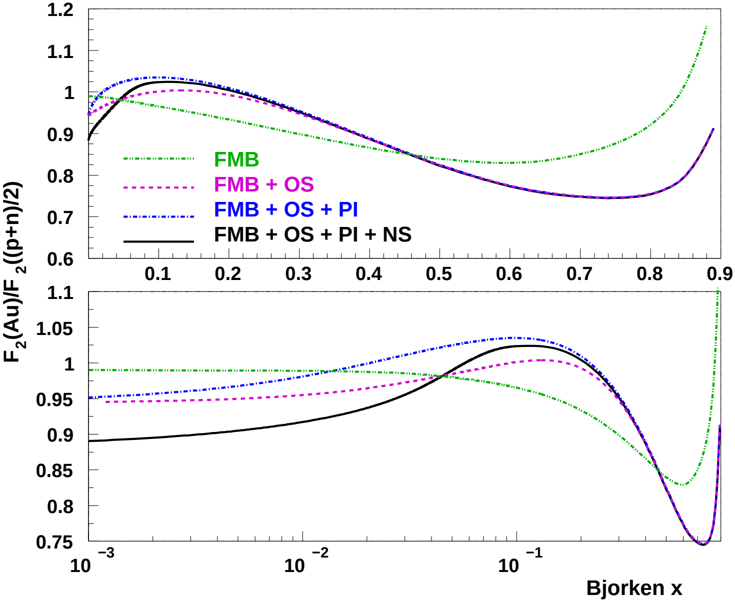

Deuteron structure functions

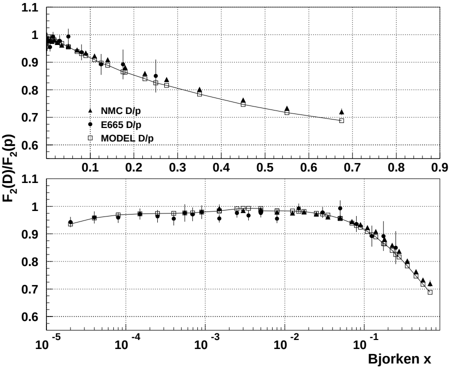

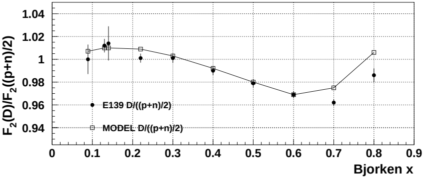

Comparison with *Gomez et.al.* extraction of $D/(p+n)$ ratio from E-139 data.

Comparison with D/p data of E665 and NMC Note that these data were not used in our fit. The data points with $x < 10^{-3}$ have $Q^2 < 0.5$ GeV^2.

Q^2 dependence of nuclear ratios

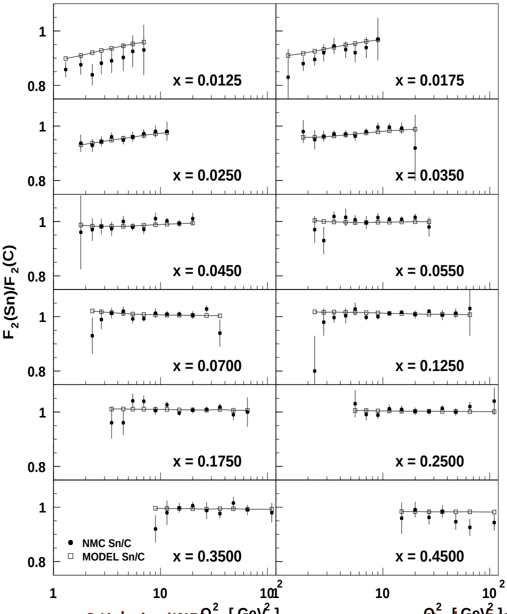

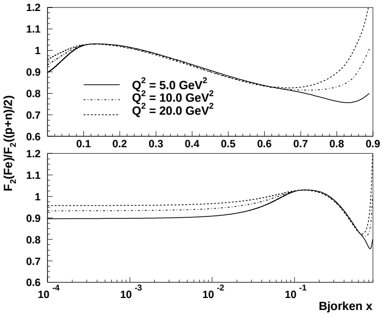

Q^2 dependence of F_2^A/F_2^D was observed for $x < 0.05$ (due to Q^2 dependence of shadowing effect) and for $x > 0.7$ (due to Q^2 dependence of target mass correction)

Comparison with E03-103 (not a fit) *S.K. & R.Petti, PRC82 (2010) 054614*

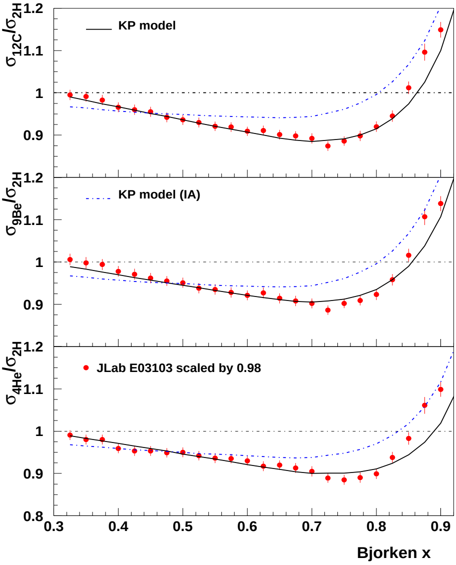

- Apply overall normalization factor 0.98 to JLab data on $^4\mathrm{He/D}$, $^9\mathrm{Be/D}$ and $^{12}\mathrm{C/D}$
- Very good agreement of our predictions with JLab E03-103 for all nuclear targets: $\chi^2/d.o.f. = 26.3/60$ for $W^2 > 2$ GeV^2
- Nuclear corrections at large x is driven by nuclear spectral function, the off-shell function $\delta f(x)$ was fixed from previous studies.
- A comparison with the Impulse Approximation (shown in blue) demonstrates that the off-shell correction is crucial to describe the data leading to both modification of the slope and position of the minimum of the EMC ratios.

Comparison with HERMES (not a fit) *S.K. & R.Petti, PRC82 (2010) 054614*

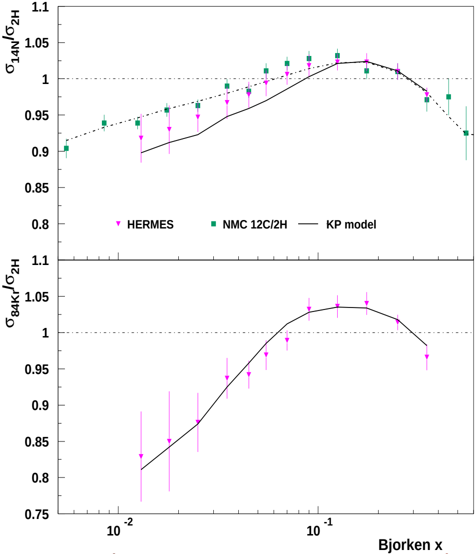

- A good agreement of our predictions with HERMES data for $^{14}\mathrm{N/D}$ and $^{84}\mathrm{Kr/D}$ with $\chi^2/d.o.f. = 14.7/24$
- A comparison with NMC data for $^{12}\mathrm{C/D}$ shows a significant Q^2 dependence at small x in the shadowing region related to the cross-section for scattering of hadronic states off the bound nucleons nucleons.

  The model correctly describes the observed x and Q^2 dependence.

The $^3\mathrm{He/D}$ and D/p data and F_2^n/F_2^p

- The $^3\mathrm{He/D}$ data allows extraction of F_2^n/F_2^p. Comparison of F_2^n/F_2^p extracted from D/p and $^3\mathrm{He/D}$ data provides a consistency test.
- D/p ratio. If we know $R_2 = F_2^D/(F_2^p + F_2^n)$ then we can extract F_2^n/F_2^p:

$$F_2^n/F_2^p = 2\mathcal{R}(\mathrm{D/p})/R_2 - 1$$

- $^3\mathrm{He/D}$ ratio. In order to extract F_2^n/F_2^p we need to know both R_2 and $R_3 = F_2^{3\mathrm{He}}/(2F_2^p + F_2^n)$:

$$F_2^n/F_2^p = (2-z)/(z-1), \text{ with } z = \tfrac{3}{2}\mathcal{R}(^3\mathrm{He/D})R_2/R_3$$

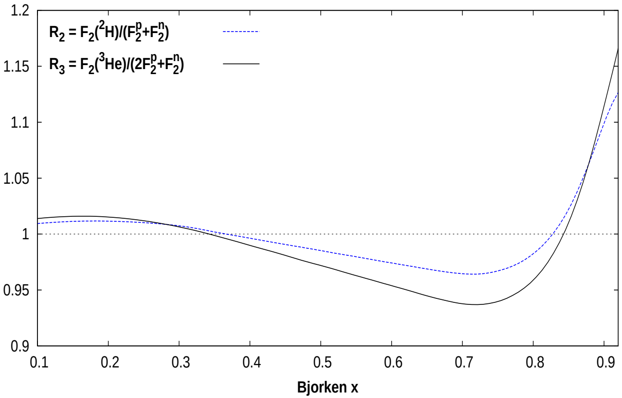

R_2 and R_3 were calculated at the values of x and Q^2 of E03-103 kinematics for $x > 0.3$ and at fixed $Q^2 = 3$ GeV^2 for $x < 0.3$.

The Paris wave function was used for the deuteron, while the Hannover spectral function was used for $^3\mathrm{He}$.

- R_2 and R_3 are similar. A dip at $x \sim 0.7$ is somewhat bigger for R_3 because of stronger binding in ^{3}He.
- Nuclear effects cancel at $x \approx 0.35$, which is consistent with the measurement of EMC effect in other nuclei.

Extraction of F_2^n/F_2^p from $^3\mathrm{He}/\mathrm{D}$ vs. D/p

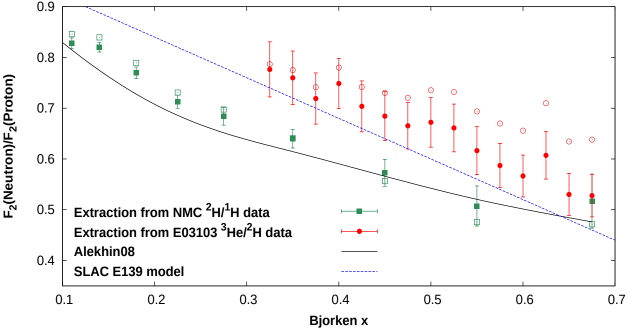

Extraction of F_2^n/F_2^p with the full treatment of nuclear effect (full symbols) and also with no nuclear effects ($R_2 = R_3 = 1$, open symbols).

- Significant mismatch in F_2^n/F_2^p extracted from different experiments. At $x \sim 0.35$, where nuclear corrections are negligible, the F_2^n/F_2^p from E03-103 is 15% higher than that from NMC.
- Normalization of F_2^n/F_2^p is directly related to normalization of $^3\mathrm{He}/\mathrm{D}$. Requiring F_2^n/F_2^p from E03-103 match NMC, we obtain a renormalization factor of $1.03^{+0.006}_{-0.008}$ for $^3\mathrm{He}/\mathrm{D}$ data.

$^3\mathrm{He/D}$ data from HERMES and JLab E03-103 experiments

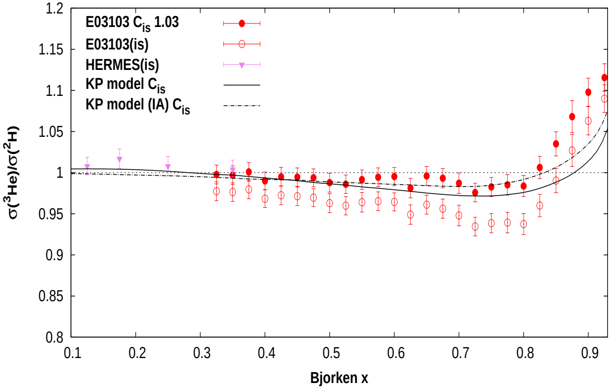

To correct for proton excess, HERMES applies the factor

$$C_{is} = \frac{AF_2^N}{ZF_2^p + NF_2^n}$$

with F_2^n/F_2^p from NMC. The E03-103 experiment does it differently, however correction factors are known.

- An unbiased way would be to compare uncorrected data, or corrected in a similar way. However, HERMES exact correction factors are lost. We uncorrect E03-103 data and then apply C_{is} together with the factor 1.03.
- After renormalization, E03-103 and HERMES data agree at the overlap ($x = 0.35$). Our calculation agree with both data (except the region $x > 0.8$).

Drell–Yan nuclear data

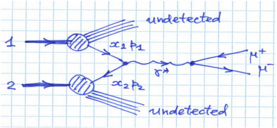

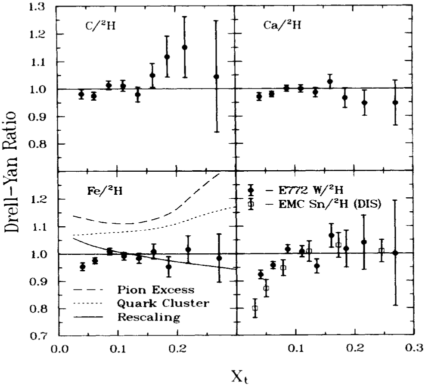

FIG. 3. Ratios of the Drell-Yan dimuon yield per nucleon, $Y_A/Y_{^2\mathrm{H}}$, for positive x_F. The curves shown for Fe/^{2}H are predictions of various models of the EMC effect. Also shown are the DIS data for Sn/^{2}H from the EMC (Ref. 4).

Drell-Yan production of a lepton pair in hadron collisions:

$$\frac{\mathrm{d}^2\sigma}{\mathrm{d}x_B\mathrm{d}x_T} = \frac{4\pi\alpha^2}{9Q^2} K \sum_a e_a^2 \left[q_a^B(x_B)\bar{q}_a^T(x_T) + \bar{q}_a^B(x_B) q_a^T(x_T)\right]$$

$$x_T x_B = Q^2/s,$$

$$x_B - x_T = 2q_L/\sqrt{s} = x_F$$

Selecting small Q^2/s and large x_F we probe the target's sea. In E772 experiment $s = 1600$ GeV^2. At $x_F = x_B - x_T > 0.2$ the process is dominated by $q^B\bar{q}^T$ annihillation. The ratio of DY yields:

$$\frac{\sigma_A^{\mathrm{DY}}}{\sigma_B^{\mathrm{DY}}} \approx \frac{\bar{q}_A(x_T)}{\bar{q}_B(x_T)}$$

Nuclear sea and valence quark distributions

Nuclear corrections for antiquark distribution $\delta\mathcal{R}_{\rm sea} = \delta\bar{q}_A/\bar{q}_N$ follow directly from nuclear corrections for C-even $q+\bar{q}$ and C-odd $q-\bar{q} = q_{\rm val}$ combinations $\delta\mathcal{R}^{(+)}$ and $\delta\mathcal{R}^{(-)}$:

$$\delta\mathcal{R}_{\rm sea} = \delta\mathcal{R}^{(+)} + \frac{q_{\rm val/N}(x)}{2\bar{q}_N(x)}\left(\delta\mathcal{R}^{(+)} - \delta\mathcal{R}^{(-)}\right)$$

$\delta\mathcal{R}_{\rm val} = \delta\mathcal{R}^{(-)}$ at $Q^2 = 20$ GeV^2 $\delta\mathcal{R}_{\rm sea}$ at $Q^2 = 20$ GeV^2

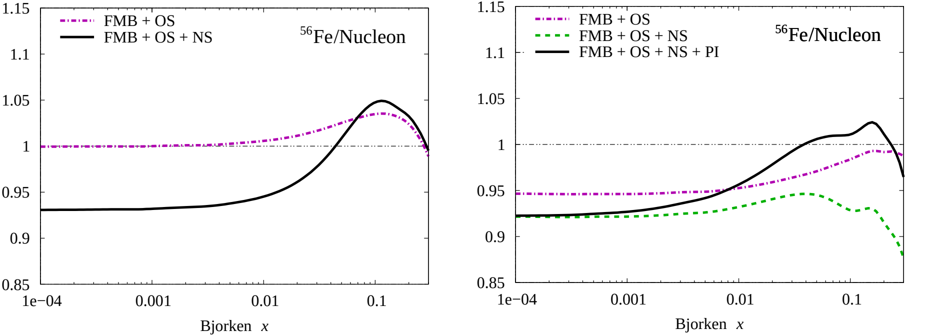

Note a remarkable cancellation between pion and shadowing effects for nuclear antiquark distribution for large $x \sim 0.1 - 0.3$.

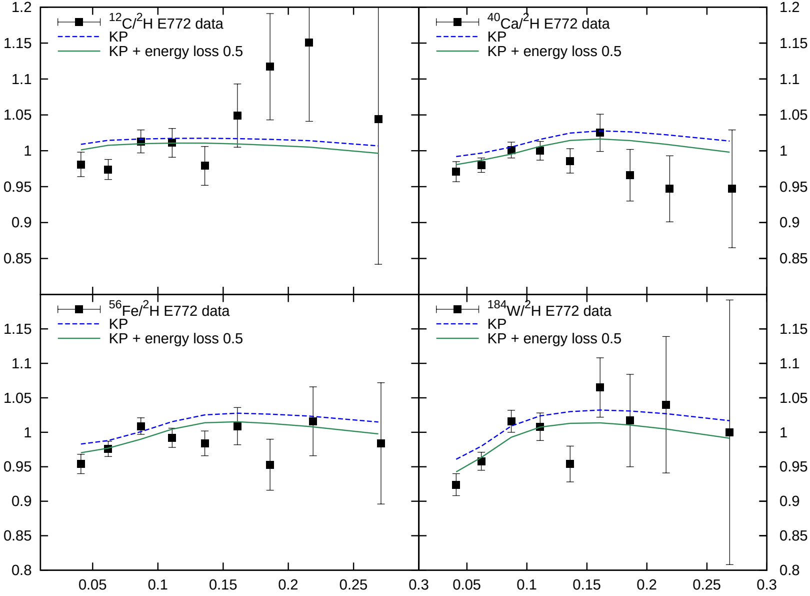

12C/2H E772 data
KP
KP + energy loss 0.5
40Ca/2H E772 data
KP
KP + energy loss 0.5
56Fe/2H E772 data
KP
KP + energy loss 0.5
184W/2H E772 data
KP
KP + energy loss 0.5

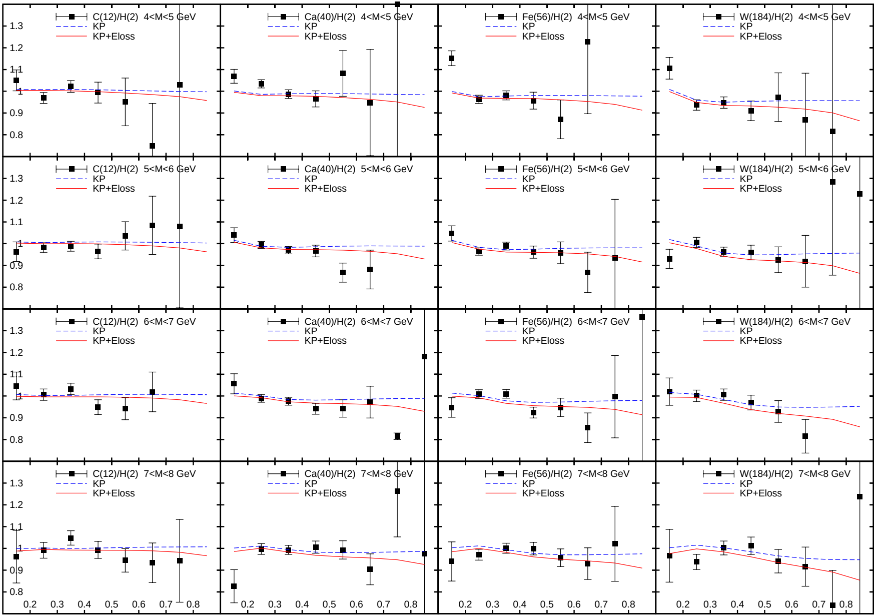
C(12)/H(2) 4<M<5 GeV
Ca(40)/H(2) 4<M<5 GeV
Fe(56)/H(2) 4<M<5 GeV
W(184)/H(2) 4<M<5 GeV
C(12)/H(2) 5<M<6 GeV
Ca(40)/H(2) 5<M<6 GeV
Fe(56)/H(2) 5<M<6 GeV
W(184)/H(2) 5<M<6 GeV
C(12)/H(2) 6<M<7 GeV
Ca(40)/H(2) 6<M<7 GeV
Fe(56)/H(2) 6<M<7 GeV
W(184)/H(2) 6<M<7 GeV
C(12)/H(2) 7<M<8 GeV
Ca(40)/H(2) 7<M<8 GeV
Fe(56)/H(2) 7<M<8 GeV
W(184)/H(2) 7<M<8 GeV
KP
KP+Eloss
1.3
1.2
1.1
1
0.9
0.8
0.2
0.3
0.4
0.5
0.6
0.7
0.8

Summary for electron DIS and DY

- A detailed semi-microscopic model of nuclear DIS was developed which includes the QCD treatment of nucleon structure function and addresses a number of nuclear effects such as shadowing, Fermi motion and nuclear binding, nuclear pion and off-shell corrections to bound nucleon structure functions
- A quantitative study of existing data from charged lepton-nucleus DIS has been performed in a wide kinematic region of x and Q^2.
- Note the importance of the nuclear binding along with the off-shell corrections to the bound nucleon structure function. The off-shell correction was extracted from data and responsible for a large fraction of nuclear effects at intermediate and large Bjorken x.
- Good agreement of our predictions with the data from JLab E03-103 and HERMES experiments.
- Good agreement with the Drell-Yan data from E772 and E866 experiments. Here we note a cancellation between different nuclear effects.

Application to neutrino scattering

Neutrino scattering is affected by both vector (V) and axial-vector (A) currents.

$$\begin{aligned} VV, AA &\quad\Longrightarrow\quad F_{1,2} \quad (\text{or } F_L,\ F_T) \\ VA &\quad\Longrightarrow\quad F_3 \text{ (not present for CL scattering)} \end{aligned}$$

Axial current is not conserved and dominates at low Q^2 (*Adler 1966*)

$$\text{PCAC:}\quad \partial A = f_\pi m_\pi^2 \varphi \quad\Longrightarrow\quad F_L = \frac{f_\pi^2 \sigma_\pi}{\pi} + \mathcal{O}(Q^2)$$

Direct contribution from the pion current $f_\pi \partial_\mu \varphi$ cancels out. Transition scale between low and high Q^2 is NOT m_π^2 but rather $M_{\text{PCAC}} \sim 1$ GeV. Model that interpolates between low and high Q^2 (*S.K. and R. Petti, PRD76,094023(2007)*):

$$F_L = \frac{f_\pi^2 \sigma_\pi}{\pi} \left(1 + \frac{Q^2}{M_{\text{PCAC}}^2}\right)^{-2} + \widetilde{F}_L$$

$$\widetilde{F}_L = \begin{cases} F_L^{\text{QCD}} & ,\ Q > 1 \text{ GeV}, \\ \propto Q^4 & ,\ Q \to 0 \end{cases}$$

The PCAC term in F_L^ν strongly affects the asymptotic behavior of $R = F_L/F_T$ as $Q^2 \to 0$

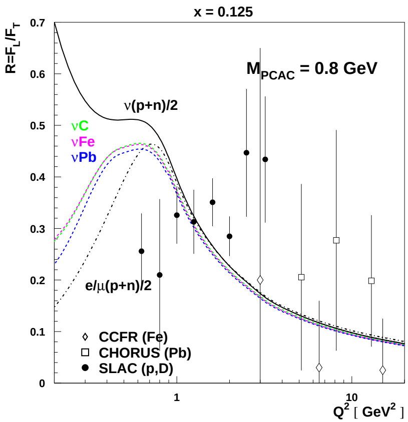

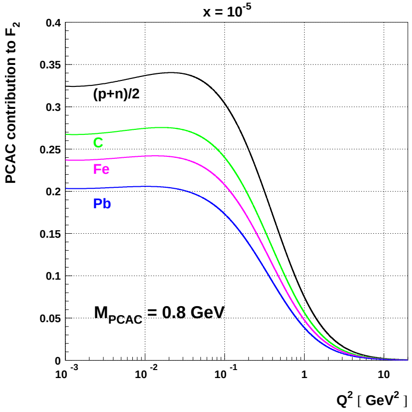

Determination for ^{56}Fe target: $F_2^\nu(Q^2 \to 0) = 0.21 \pm 0.02$ by *CCFR Coll. PRL 86 (2001) 5430*

Nuclear effects F_2 vs. xF_3

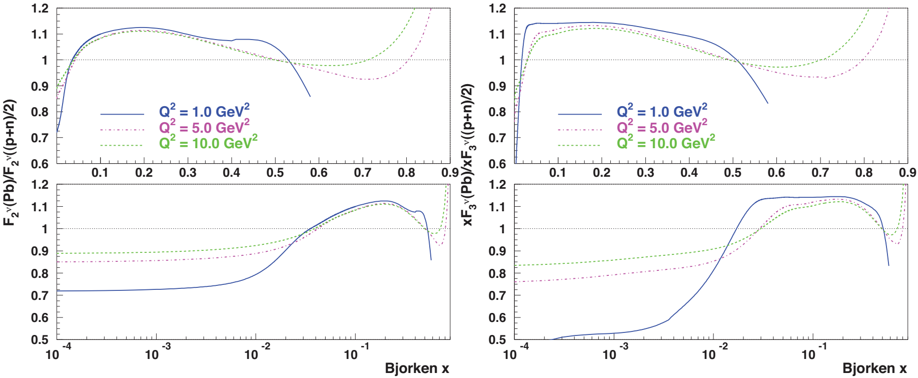

Ratio of Charged Current structure functions on ^{207}Pb and isoscalar nucleon $(p+n)/2$

Nuclear effects for ν vs. $\bar{\nu}$

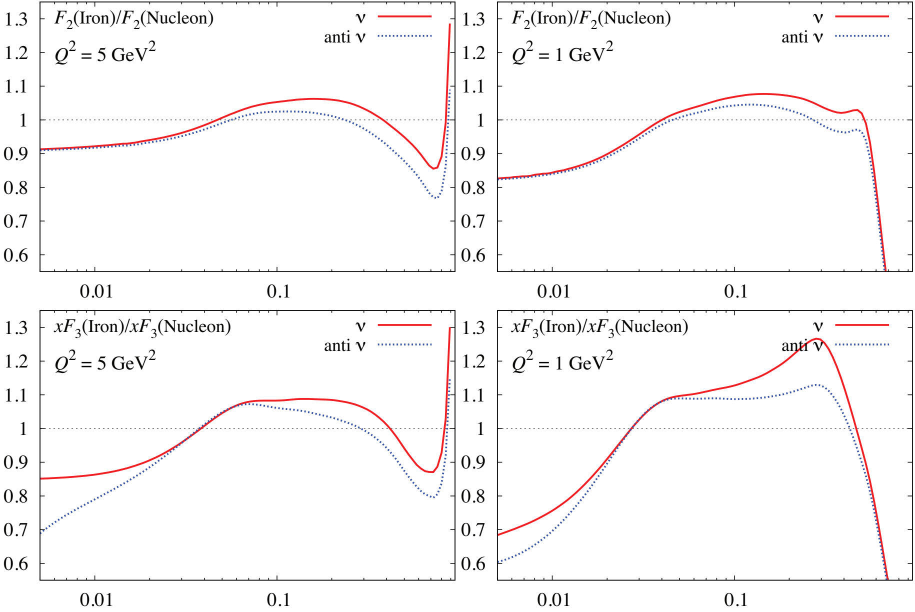

Isoscalar vs. isovector nuclear effects

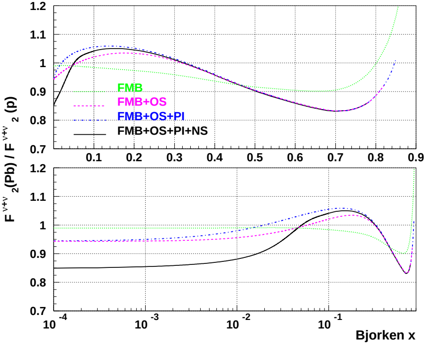

The ratio $\frac{1}{A}F_2^{(\nu+\bar{\nu})A}/F_2^{(\nu+\bar{\nu})p}$ calculated for ^{207}Pb at $Q^2 = 5$ GeV^2. The labels on the curves correspond to effects due to Fermi motion and nuclear binding (FMB), off-shell correction (OS), nuclear pion excess (PI) and coherent nuclear processes (NS).

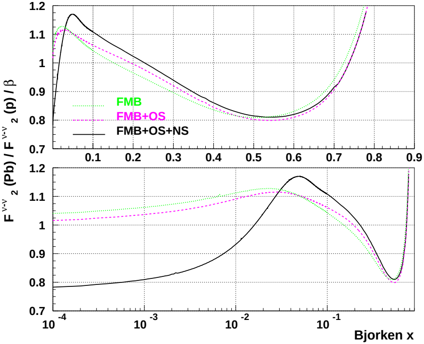

The ratio $\frac{1}{A}F_2^{(\nu-\bar{\nu})A}/(\beta F_2^{(\nu-\bar{\nu})p})$ calculated for ^{207}Pb at $Q^2 = 5$ GeV^2. The labels on the curves correspond to effects due to Fermi motion and nuclear binding (FMB), off-shell correction (OS) and coherent nuclear processes (NS).

BEBC measurement

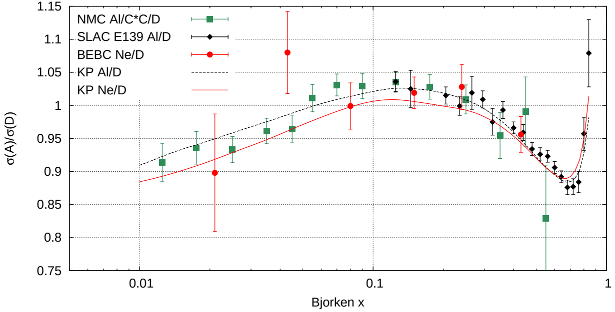

- So far the only DIRECT measurement of nuclear effects in $\nu(\bar{\nu})$ DIS from ratio ^{20}Ne/D by *BEBC Coll., ZPC 36 (1987) 337; PLB 232 (1989) 417*
  - Consistent with shadowing at small x_{Bj} but large uncertainties;
  - Consistent with the EMC effect measured from e, μ DIS.
- Differences with respect to e, μ DIS at small x mainly due to the axial-vector current.

Neutrino cross sections

(Anti)neutrino differential cross sections in terms of Bjorken x and inelasticity y:

$$\frac{\mathrm{d}^2\sigma_{\mathrm{CC}}^{(\nu,\bar\nu)}}{\mathrm{d}x\mathrm{d}y} = \frac{G_F^2 M E}{\pi(1+Q^2/M_W^2)^2}\left[Y_+ F_2^{\nu,\bar\nu} - y^2 x F_L^{\nu,\bar\nu} \pm Y_- x F_3^{\nu,\bar\nu}\right],$$

$$Y_+ = \frac{1}{2}\left[1+(1-y)^2\right] + M^2x^2y^2/Q^2, \quad Y_- = \frac{1}{2}\left[1-(1-y)^2\right].$$

Recently published cross-section data:

NuTeV data on $^{56}\mathrm{Fe}$:
about $1400\nu + 1200\bar\nu$ data points for $35 < E < 340$ GeV, $0.015 < x < 0.75$, $0.05 < y < 0.95$.

CHORUS data on $^{208}\mathrm{Pb}$:
about $600\nu + 600\bar\nu$ data points for $25 < E < 170$ GeV, $0.02 < x < 0.65$, $0.1 < y < 0.8$.

Comparison with CHORUS and NuTeV cross sections

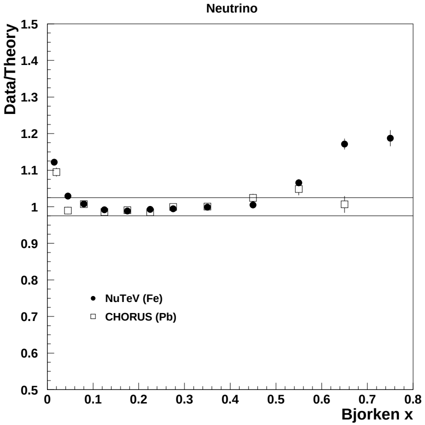

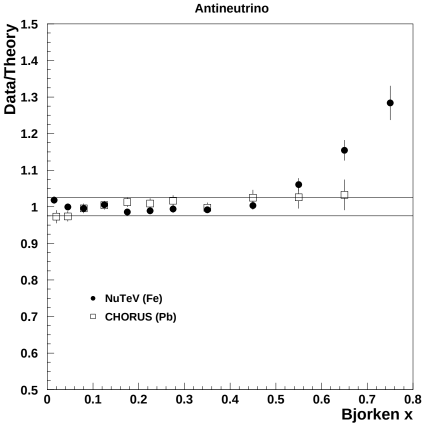

Data/model predictions by *S.K. and R.Petti, NPA 765 (2006) 126; PRD 76 (2007) 094023*. The x-point is the weighted average over available E and y. The solid horizontal lines indicate a $\pm 2.5\%$ band.

χ^2 analysis (not a FIT)

Cut	No. of data points Neutrino	Antineutrino	χ^2/d.o.f. Neutrino	Antineutrino
NuTeV (^{56}Fe)				
No cut	1423	1195	1.36	1.10
$x > 0.015$	1324	1100	1.15	1.08
$x < 0.55$	738	671	1.16	1.02
$0.015 < x < 0.55$	686	620	0.97	1.01
CHORUS (^{208}Pb)				
No cut	607	607	0.68	0.84
$x > 0.02$	550	546	0.55	0.83
$x < 0.55$	506	507	0.74	0.83
$0.02 < x < 0.55$	449	447	0.60	0.83

- Good agreement with CHORUS differential cross section data for $^{208}\mathrm{Pb}$ in the whole kinematical range.
- Good agreement with NuTeV cross sections for $^{56}\mathrm{Fe}$ for $0.015 < x < 0.55$.
- Excess of data/theory for NuTeV cross sections at large $x > 0.5$ for both ν and $\bar{\nu}$. No such excess for CHORUS(Pb) (and also NOMAD(Fe) data – *Roberto Petti, private communication*).
- Excess of data over theory for both, NuTeV and CHORUS data at small x ($0.015 - 0.025$) (also supported by preliminary NOMAD(Fe) data – *Roberto Petti, private communication*).

Summary for neutrino nuclear DIS

- The presence of a nonconserved axial-vector current is important difference with respect to the charged-lepton DIS. A low-Q^2 region in neutrino scattering is driven by the axial current contribution. Note that for that reason the ratio $R = F_L/F_T$ for neutrino interaction is crucially different from that of the charged-lepton scattering.
- The nuclear corrections depend on the type of the structure function (F_2 vs xF_3). The nuclear corrections are also different for the isoscalar $F_2^{\nu+\bar{\nu}}$ and the isovector $F_2^{\nu-\bar{\nu}}$ combinations.
- Predictions for neutrino cross sections are in a good agreement (within $\pm 2.5\%$ band) with the CHORUS $^{208}\mathrm{Pb}$ data in the whole kinematical region of x and Q^2. We also observe a good agreement with the NuTeV $^{56}\mathrm{Fe}$ data in the region $0.15 < x < 0.55$.
- Note systematic excess of data/theory for the NuTeV data at large $x > 0.5$ for both the neutrino and antineutrino.
- Note also about 10% data/theory excess for small $x = 0.015$ for neutrino scattering for both the $^{208}\mathrm{Pb}$ and $^{56}\mathrm{Fe}$ data.

Backup

Targets	χ^2/DOF						
	NMC	EMC	E139	E140	BCDMS	E665	HERMES
$^4\mathrm{He}/^2\mathrm{H}$	10.8/17		6.2/21				
$^7\mathrm{Li}/^2\mathrm{H}$	28.6/17						
$^9\mathrm{Be}/^2\mathrm{H}$			12.3/21				
$^{12}\mathrm{C}/^2\mathrm{H}$	14.6/17		13.0/17				
$^9\mathrm{Be}/^{12}\mathrm{C}$	5.3/15						
$^{12}\mathrm{C}/^7\mathrm{Li}$	41.0/24						
$^{14}\mathrm{N}/^2\mathrm{H}$							9.8/12
$^{27}\mathrm{Al}/^2\mathrm{H}$			14.8/21				
$^{27}\mathrm{Al}/^{12}\mathrm{C}$	5.7/15						
$^{40}\mathrm{Ca}/^2\mathrm{H}$	27.2/16		14.3/17				
$^{40}\mathrm{Ca}/^7\mathrm{Li}$	35.6/24						
$^{40}\mathrm{Ca}/^{12}\mathrm{C}$	31.8/24					1.0/5	
$^{56}\mathrm{Fe}/^2\mathrm{H}$			18.4/23	4.5/8	14.8/10		
$^{56}\mathrm{Fe}/^{12}\mathrm{C}$	10.3/15						
$^{63}\mathrm{Cu}/^2\mathrm{H}$		7.8/10					
$^{84}\mathrm{Kr}/^2\mathrm{H}$							4.9/12
$^{108}\mathrm{Ag}/^2\mathrm{H}$			14.9/17				
$^{119}\mathrm{Sn}/^{12}\mathrm{C}$	94.9/161						
$^{197}\mathrm{Au}/^2\mathrm{H}$			18.2/21	2.4/1			
$^{207}\mathrm{Pb}/^2\mathrm{H}$						5.0/5	
$^{207}\mathrm{Pb}/^{12}\mathrm{C}$	6.1/15					0.2/5	

Values of χ^2/DOF between different data sets with $Q^2 \geq 1$ GeV^2 and the predictions of KP model *NPA765(2006)126; PRC82(2010)054614*. The sum over all data results in $\chi^2/\mathrm{DOF} = 466.6/586$.

Off-shell effect and the bound nucleon radius

The valence quark distribution in (off-shell) nucleon (see, e.g., *Kulagin, Piller & Weise, PRC* **50**, *1154 (1994)*)

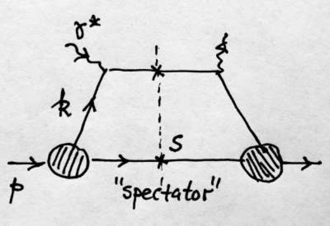

$$q_{\mathsf{val}}(x,p^2) = \int^{k^2_{\mathsf{max}}} \mathrm{d}k^2 \Phi(k^2,p^2)$$

$$k^2_{\mathsf{max}} = x\left(p^2 - s/(1-x)\right)$$

- A one-scale model of quark k^2 distribution: $\Phi(k^2) = C\phi(k^2/\Lambda^2)/\Lambda^2$, where C and ϕ are dimensionless and Λ is the scale.
- Off-shell: $C \to C(p^2),\ \Lambda \to \Lambda(p^2)$
- The derivatives $\partial_x q_{\mathsf{val}}$ and $\partial_{p^2} q_{\mathsf{val}}$ are related

$$\delta f(x) = \frac{\partial \ln q_{\mathsf{val}}}{\partial \ln p^2} = c + \frac{\mathrm{d}q_{\mathsf{val}}(x)}{\mathrm{d}x} x(1-x)h(x)$$

$$h(x) = \frac{(1-\lambda)(1-x) + \lambda s/M^2}{(1-x)^2 - s/M^2}$$

$$c = \frac{\partial \ln C}{\partial \ln p^2},\quad \lambda = \frac{\partial \ln \Lambda^2}{\partial \ln p^2}$$

- A simple pole model $\phi(y) = (1-y)^{-n}$ (note that $y < 0$ so we do not run into singularity) provides a resonable description of the nucleon valence distribution for $x > 0.2$ and large Q^2 ($s = 2.1$ GeV^2, $\Lambda^2 = 1.2$ GeV^2, $n = 4.4$ at $Q^2 = 15 \div 30$ GeV^2).
- The size of the valence quark confinement region $R_c \sim \Lambda^{-1}$ (nucleon core radius).
- Off-shell corection is independent of specific choice of profile $\phi(y)$ and is given by $(\ln q_{\mathsf{val}}(x))'$.
- Fix c and λ to reproduce $\delta f_2(x_0) = 0$ and the slope $\delta f_2'(x_0)$.
We obtain $\lambda \approx 1$ and $c \approx -2.3$. The positive parameter λ suggests decreasing the scale Λ in nuclear environment (swelling of a bound nucleon)

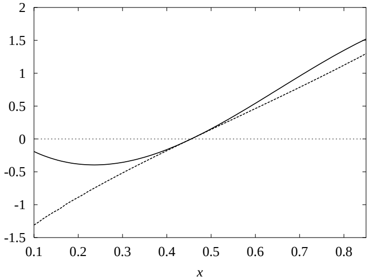

$$\frac{\delta R_c}{R_c} \sim -\frac{1}{2}\frac{\delta\Lambda^2}{\Lambda^2} = -\frac{1}{2}\lambda\frac{\langle p^2 - M^2\rangle}{M^2}$$

^{56}Fe : $\delta R_c/R_c \sim 9\%$

^{2}H : $\delta R_c/R_c \sim 2\%$